OPTIMAL DETECTION AND TRACKING OF ACOUSTICAL NOISE SOURCES IN A TIME-VARYING ENVIRONMENT

by

Hendrik Van Asselt
SACLANT ASW Research Centre
La Spezia, Italy

ABSTRACT

A dynamical detector estimator is derived for nonlinear nongaussian signal processes based on Bucy's representation theorem which is the fundamental result in stochastic filtering. A quantized version of two-dimensional conditional probability density functions is generated for bearing and bearing-rate as well as for frequency and frequency-rate. Results of the analysis of real data for bearing and bearing rate are presented and discussed using optimal nonlinear filtering techniques.

INTRODUCTION

Target detection and tracking from passive sensors is a nonlinear estimation problem and has practical significance. This paper discusses this problem and presents an analysis of real target data measured in shallow water.

The present state of the art makes it feasible to develop detection and estimation algorithms in discrete time, since nonlinear processing algorithms based on Bayes law are developed in discrete time.

In this paper we have restricted ourselves to hardware that is available today, which means that the closeness of approximations to optimality depends largely on the dimensionality of the signal processes.

We have divided our system into two parts, bearing and frequency estimators, which each turn out to be two-dimensional dynamical processes having nonlinear system functions and linear observation functions. Because of the lower dimensionality of bearing and frequency , when the state spaces are decoupled, one can use a more accurate approximation to optimality than for the coupled state/space representation if one thinks in terms of the number of computations required and of the real-time implementation.

For bearing and frequency estimation we are able to generate quantized versions of two-dimensional conditional probability density functions and represent these as a set of point masses on a moving mesh. A detailed discussion is given in <1>.

Our motivation for this type of data-processing scheme is that the nature of most signals relating to passive sonar detection and tracking are multidimensional signal processes and are commonly dynamical, nonlinear, and nongaussian and, further, may have time-varying statistics. "Classical" signal-processing schemes based on the stationary steady-state filtering theory therefore often give undesired performance, especially in cases of low signal-to-noise ratios.

1 SYSTEMS CONSIDERATIONS

Kalman filtering is often applied for designing suboptimal nonlinear estimators. The procedure is that the models are linearized and then the linear theory is applied. This is one of the simplest methods of deriving suboptimal data-processing schemes for nonlinear dynamical signal processes. Often, however, these techniques lead to undesirable performance, as we will illustrate in a simple example.

Figure 1 compares a recursive realization of the kalman filter with the discrete Bayes-Law estimator for the case of truncated gaussian densities. The a-priori conditional probability density function is indicated by $\hat{\mu}_{n-1}$ having a variance $\hat{P}_{n-1} = 0.6$. The probability density function of the observations Z_n has a variance $R_n = 1.2$ and the system noise has a probability density function m and variance $Q_n = 0.696$.

If we calculate the a posteriori conditional probability density function, then both the kalman estimator and the Bayes-Law estimator provide almost the same output variance: $\hat{P}_B = 0.6$ and $P_k = 0.62$. The difference results from the fact that Bayes Law computes on the real truncated gaussian densities whereas the kalman filter assumes non-truncated densities.

Figure 2 makes the same comparison. Consider now $\hat{\mu}_{n-1}$; the real a-priori conditional probability density function is nongaussian, whereas the kalman filter assumes it is gaussian, both having the same variance. Also the real probability density function Z of the input data is nongaussian and again the kalman filter assumes it is gaussian.

Comparing the results of this example we note that a kalman filter severely underestimates the conditional a-posteriori variance. As a consequence it will also severely underestimate the filter gain matrix. This causes too little information to be extracted from the measurements, leading frequently to divergence. This, of course, is not to blame the kalman filter, it is a result of its wrong application.

1.1 Implementation of a Bayes-Law System

Figure 3 shows the configuration of a Bayes-Law system. The input is obtained from a line array of 20 hydrophones approximately 2 m apart. This is followed by a conventional beamformer in order to sample the noise field passively. The beam-axes are 1° apart and the beamwidth is 5° at the 3 dB level.

All the beams do not necessarily carry the same levels of energy and the energy levels per beam fluctuate within a range of approximately 10 dB.

Along the array we observe the signal, which is "more or less" coherent. We cannot specify a measure of coherence, because it is not a constant. After beamforming we could observe this as presented in Fig. 4. The shaded zone shows the collection of 2000 beamformer output samples, where we have eliminated time dependence. If this shadowed zone were to collapse to a broken line we would receive a fully coherent signal; so a measure of noncoherence is indicated by the width of the shaded area. Note also that the noise field is nonhomogeneous.

Given these sample functions we then evaluate the likelihood function in order to generate a probabilistic structure in space.

In Fig. 3 these observations are indicated as $Z[h(\xi), G(\xi)]$, where $h(\xi)$ is the input function and $G(\xi)$ the array gain in a given direction. We then continue by two-dimensionally convolving the probabilistic structure described above with the product of the probability density function $m[y, f(\xi), r]$ describing the target trajectory noise and the a-priori conditional probability density function $\hat{D}_{n-1}(\xi)$ (see also Ch. 4 of <2>, especially pp 43-59).

We have m modelled as a gaussian density function, the arguments y (and dummy ξ) describing the target-motion variables in state/space (bearing, bearing rate and frequency, frequency rate) and the target-motion model represented by $f(\xi)$, where τ is the average manoeuvring time. During the detection phase the target motion is modelled as a linear trajectory in cartesian coordinates having random accelerations (the constant-speed model). During the tracking phase we use a constant-acceleration model in order to allow target manoeuvring. This can be achieved by changing the autocorrelation time.

After we have generated the conditional probability density function, it is simple to compute mean values and variances, as is indicated in Fig. 3. Figure 5 presents the estimated variances of a) bearing and b) bearing-rate and shows the potential of the nonlinear optimal estimator.

Figure 6 shows a typical example, where the dynamics behave reasonably stationary. We cut the density function into two halves along the correlation axis in order to study its transient during the detection phase (Fig. 4). At the start, t_o, we have no information, which is represented by a uniform initial probability density $\hat{D}(t_o)$. Then at intervals of 2 seconds we update the estimated density $\hat{D}(\ )$, e.g. t_5 refers to 10 seconds processing time. We stop the detection phase after t_8, which is where the detector has reached the steady-state solution. Table 1 presents the detector performance numerically, with reference to the highest level, which is at 91° and zero degrees per second. After the detection phase the autocorrelation time of the target accelerations is increased so that the transient is observed from detection to tracking phase. Figure 7 shows a sequence of pictures showing both transients. Figure 8 is another example, in which the estimators have been left in the detection mode so as to show the detectors capability of handling dynamical processes (a relative fast ship moving through a fixed set of beams).

A sequence of 2000 sequentially estimated conditional probability densities has been filmed to show in more detail the systems dynamics. This pictorial display demonstrates why techniques based on stationary steady-state filtering theory cannot work properly. This is because often averaging time is too long with respect to the non-stationarity of the underlying signal-process <3>.

2 DETECTOR DERIVATION

The stochastical differential equation representing a diffusion process is:

$$dx_t = f(x_t, t)dt + \sigma(x_t, t)du_t \ , \qquad \text{(Eq. 1)}$$

where x_t, u_t and $f(x_t, t)$ are n-dimensional vectors

and $\sigma(x_t, t)$ is an $n \times n$ matrix.

Assume that a solution exists and is unique and that the domain of the solution will be the bounded time interval [a, b]. The process $\{u_t\} = \{(u_{1,t}, u_{2,t} \cdots\cdots u_{n,t})^T\}$ defines the vector of n independent Brownian motions. The components of $f(x_t,t)$ and $\sigma(x_t,t)$ are continuous in t and Lipschitz-continuous in x_t.

For the m-dimensional observation process we use the differential equations

$$\begin{aligned} dz_t &= h(x_t, t)dt + \gamma(t)dv_t \quad && \text{signal present} \\ dz_t &= \gamma(t)dv_t && \text{signal absent} \end{aligned} \qquad \text{(Eq. 2)}$$

where dx_t is defined in Eq. 1,

$$\begin{aligned} &x(a) = c, \\ &z(a) = 0, \\ &v_t \text{ is an m-dimensional Brownian motion, independent of } u_t. \end{aligned} \qquad \text{(Eq. 3)}$$

Then, following <4>, consider

$$dx_t = f(x_t, t)dt + \sigma(x_t, t)du_t \qquad \text{(Eq. 4)}$$

$$dz_t = [f(x_t, t) + \sigma(z_t, t)\, \gamma(z_t, t)]dt + \sigma(z_t, t)du_t \ , \qquad \text{(Eq. 5)}$$

where $t \in [a, b]$ $\qquad x(a) = z(a)$

f, γ are n-vectors and σ is an $n \times n$ matrix

f, σ and γ are measurable in both arguments

$$\int_a^{\ell} \left| \gamma(x_t,t) \right|^2 dt < \infty \qquad \text{w.p.1}$$

$|\gamma(x_t,t)| < \gamma_o(|x_t|)$; γ_o being a nondecreasing function of a real variable.

Then the measures m_x and m_z induced on the space of all continuous functions in $\mathbb{R}^n, C_n[a,b]$ by the processes $\{x_t\}$ and $\{z_t\}$ are mutually absolute continuous. The Radon-Nikodym derivative dm_x/dm_z is then given by

$$\frac{dm_x}{dm_z} = \exp\left[\int_a^b \gamma^T(x_s,s)dv_s - \frac{1}{2}\int_a^b |\gamma(x_s,s)|^2 ds\right] \qquad \text{(Eq. 6)}$$

The nonlinear detection and estimation problem is described <2> by:

$$dx_t = f(x_t,t)dt + \sigma(x_t,t)du_t \qquad \text{(Eq. 7)}$$

$$dz_t = h(t)x_t dt + \gamma(t)dv_t \qquad \text{(Eq. 8)}$$

The conditional mean for this estimation problem is given by

$$E[x_t \mid z_r; a \le r \le t] = \hat{x}_t = \frac{E_{mx}[\Omega_t X_t]}{E_{mx}[\Omega_t]} \qquad \text{(Eq. 9)}$$

The expectation symbol E_{mx} defines integration with respect to the function space measure m_x generated by solving Eq. 7 and

$$\Omega_t = \Omega_t(x_r,z_r;\ a \le t \le r) =$$

$$\exp\left[\int_a^t x_r^T h_r^T [\gamma_r^T \gamma_r]^{-1} dz_r - \tfrac{1}{2}\int_a^t x_r^T h_r^T [\gamma_r^T \gamma_r]^{-1} h_r x_r dr\right]$$

Recalling the detection problem of Eq. 2 and defining the process $\{P_t\}$ as

$$P_t = \ell n\, E_{mx}[\Omega_t],$$

which satisfies the stochastic differential equation

$$dP_t = \hat{x}_t^T h_t^T [\gamma_t^T \gamma_t]^{-1} dz_t - \tfrac{1}{2}\hat{x}_t^T h_t^T [\gamma_t^T \gamma_t]^{-1} h_t \hat{x}_t\, dt, \qquad \text{(Eq. 10)}$$

where $\hat{x}_t$ is given by Eq. 9.

This can be proved because $E_{mx}[\Omega_t]$ is positive and finite w.p. 1; therefore P_t is well defined. If we apply the stochastic differential rule to $\ell n\, E_{mx}[\Omega_t]$ we obtain

$$dP_t = \frac{E_{mx}[x_t^T h_t^T \{\gamma_t^T \gamma_t\}^{-1} \Omega_t] dz_t}{E_{mx}[\Omega_t]} +$$

$$- \tfrac{1}{2}\frac{E_{mx}[x_t^T h_t^T \Omega_t]\ \{\gamma_t^T \gamma_t\}^{-1}\ E_{mx}[h_t x_t \Omega_t]}{\{E_{mx}[\Omega_t]\}^2}$$

and we find the likelihood function

$$dP_t = \hat{x}_t^T h_t^T [\gamma_t^T \gamma_t]^{-1} \, dz_t +$$
$$- \tfrac{1}{2} \hat{x}_t^T h_t^T [\gamma_t^T \gamma_t]^{-1} \, h_t \, \hat{x}_t \, dt$$

This concludes our detection process for a diffusion process in white noise.

CONCLUSIONS

A dynamical detector/estimator is presented for nonlinear nongaussian signal processers. We have shown the performance of the bearing/bearing rate estimator where the input was real data.

REFERENCES

1. BUCY, R.S. and SENNE, K.D. Digital synthesis of non-linear filters, Automatica, 7, 1981: 287-298.

2. BUCY, J. Filtering for stochastic processes with applications to guidance. New York, N.Y., Interscience publishers, John Wiley and Sons, 1968.

3. UMAPATH Reddy V., EGARDT, B. and KAILATH, T. Optimized lattice form adaptive line enhancer for a sinusoidal signal in broadband noise, IEEE Transactions, Acoustics, Speech and Signal Processing, 29, 1981: 702-710.

4. GIRSANOV, I.V. On transforming a certain class of stochastic processes by absolutely continuous substitution of measures, 1960.

ADDITIONAL BIBLIOGRAPHY

ITO, K. Lectures on stochastic processes. Tata Institute for Fundamental Research, 1961.

STRATONOVICH, R.L. A new representation for stochastic integrals (English translation). SIAM Journal on Control and Optimization, 4, 1966: 362-371.

SOSULIN, STRATONOVICH. Optimum detection of a diffusion process in white noise (English translation). Radio Engineering and Electronic Physics, 10, 1965: 704-714.

KALMAN, R.E. and BUCY, R.S. New results in linear filtering theory. Journal Basic Engineering (ASME TRANS), 83, 1961: 95-108.

TRUNCATED GAUSSIAN EXAMPLE FOR LINEAR SCALAR SYSTEM

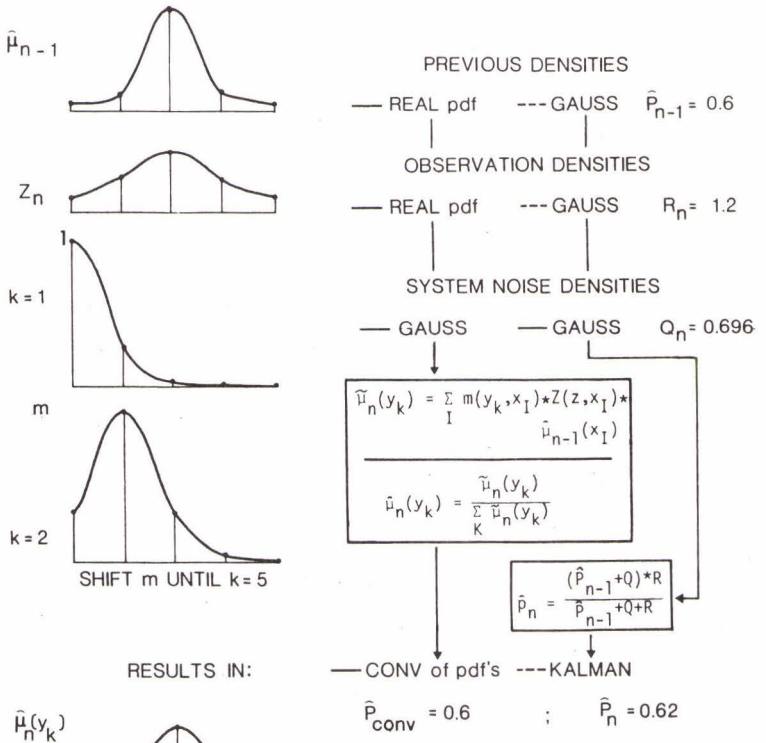

FIG. 1

NON-GAUSSIAN EXAMPLE FOR LINEAR SCALAR SYSTEM

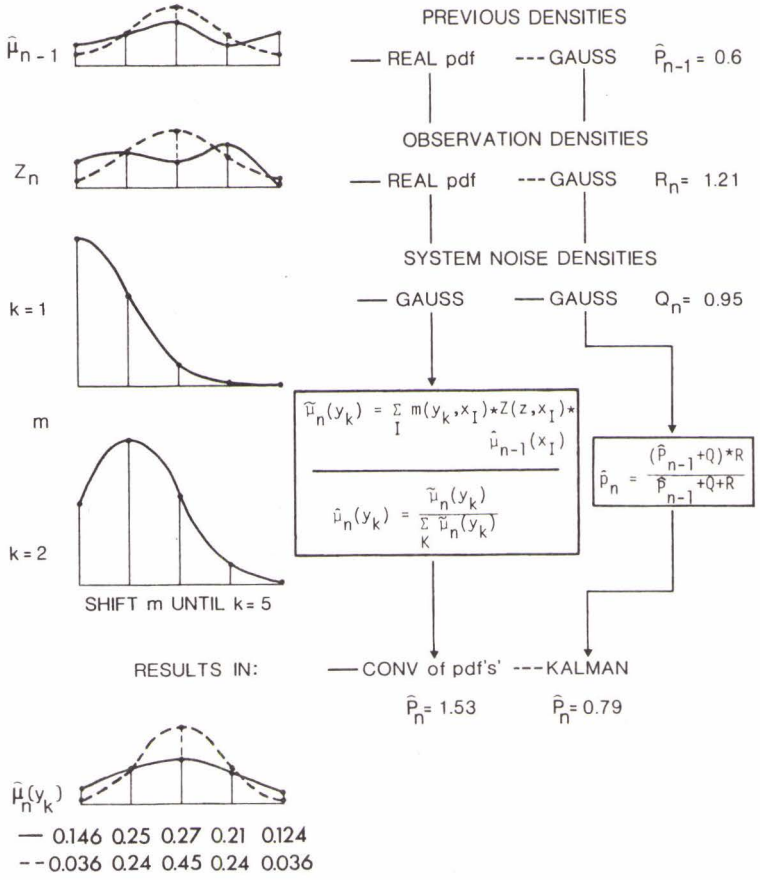

FIG. 2

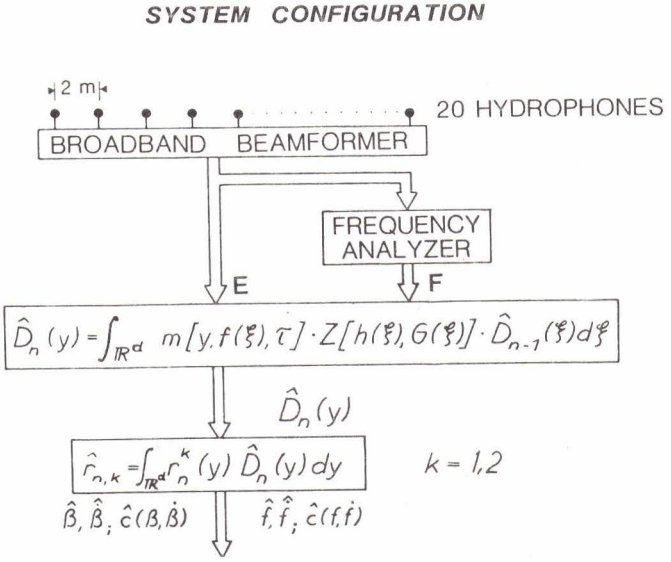
SYSTEM CONFIGURATION
2 m
20 HYDROPHONES
BROADBAND BEAMFORMER
FREQUENCY ANALYZER
E
F
$\hat{D}_n(y) = \int_{IR^d} m[y, f(\xi), \tau] \cdot Z[h(\xi), G(\xi)] \cdot \hat{D}_{n-1}(\xi) d\xi$
$\hat{D}_n(y)$
$\hat{r}_{n,k} = \int_{IR^d} r_n^k(y)\, \hat{D}_n(y)\, dy$
$k = 1,2$
$\hat{\beta}, \dot{\hat{\beta}}; \hat{c}(\beta, \dot{\beta})$
$\hat{f}, \dot{\hat{f}}; \hat{c}(f, \dot{f})$

FIG. 3

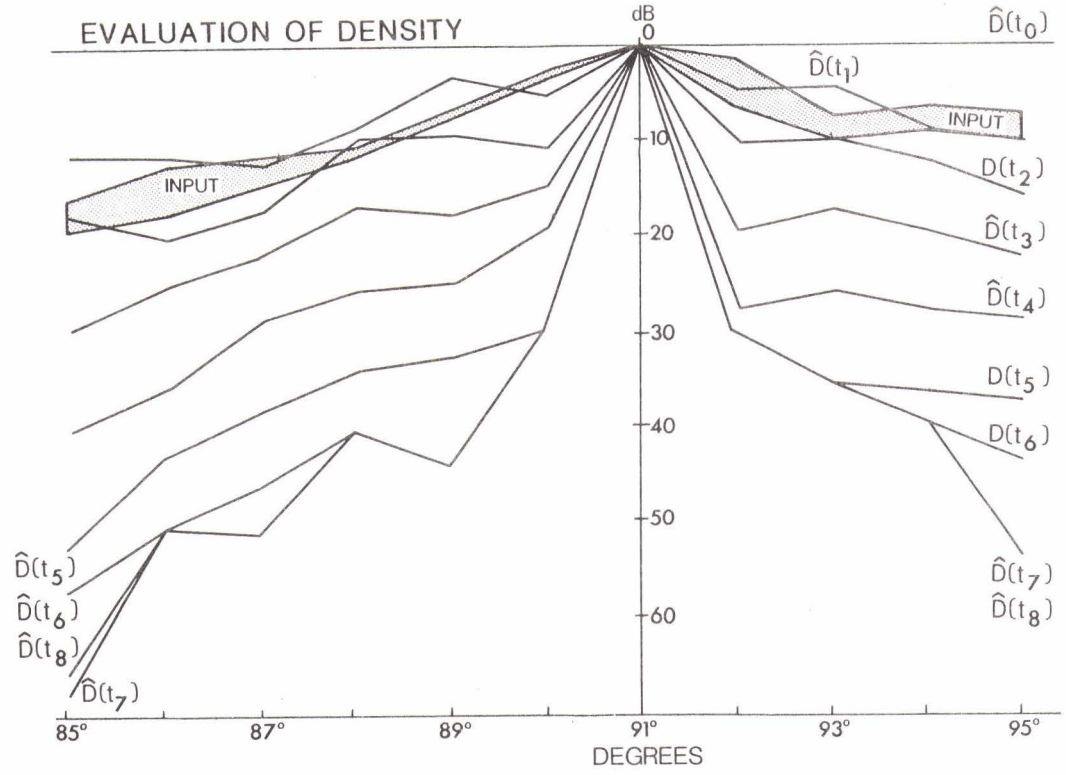
EVALUATION OF DENSITY
dB
0
10
20
30
40
50
60
INPUT
INPUT
$\hat{D}(t_0)$
$\hat{D}(t_1)$
$D(t_2)$
$\hat{D}(t_3)$
$\hat{D}(t_4)$
$D(t_5)$
$D(t_6)$
$\hat{D}(t_7)$
$\hat{D}(t_8)$
$\hat{D}(t_5)$
$\hat{D}(t_6)$
$\hat{D}(t_8)$
$\hat{D}(t_7)$
85°
87°
89°
91°
93°
95°
DEGREES

FIG. 4

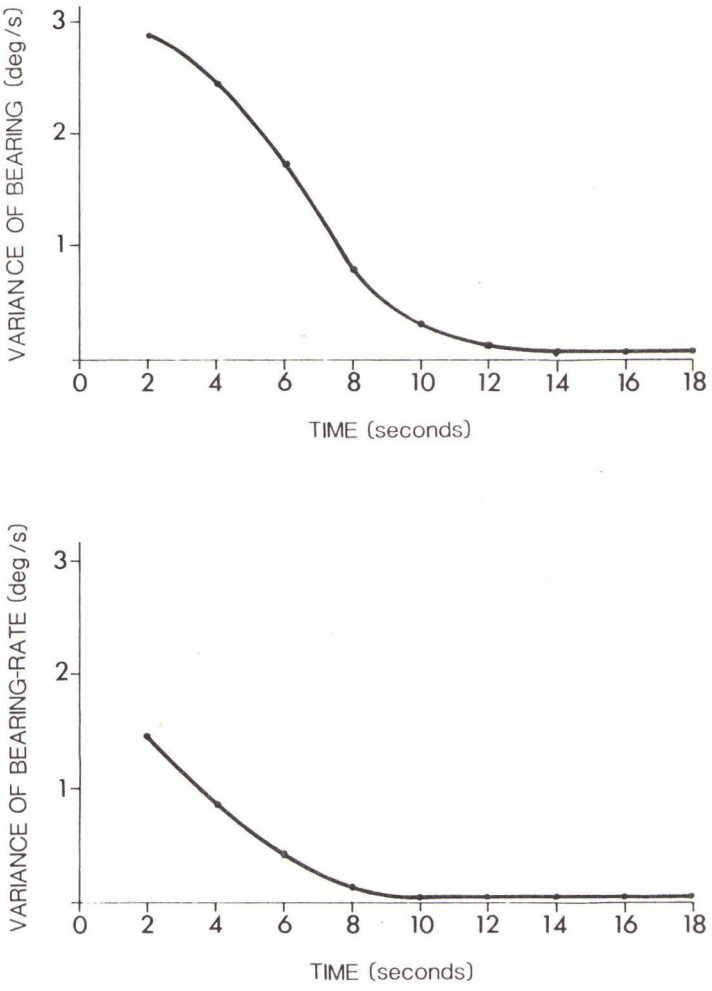

FIG. 5

QUANTIZED CONDITIONAL PROBABILITY DENSITY FUNCTION

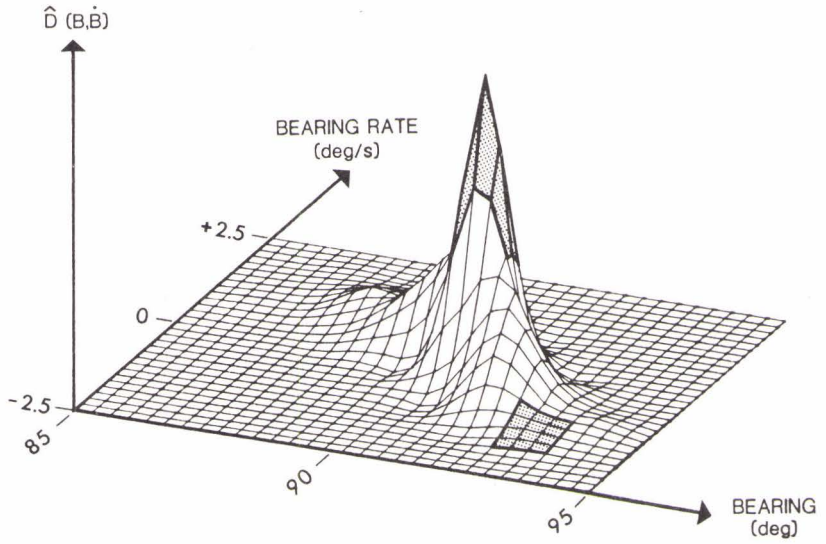

FIG. 6

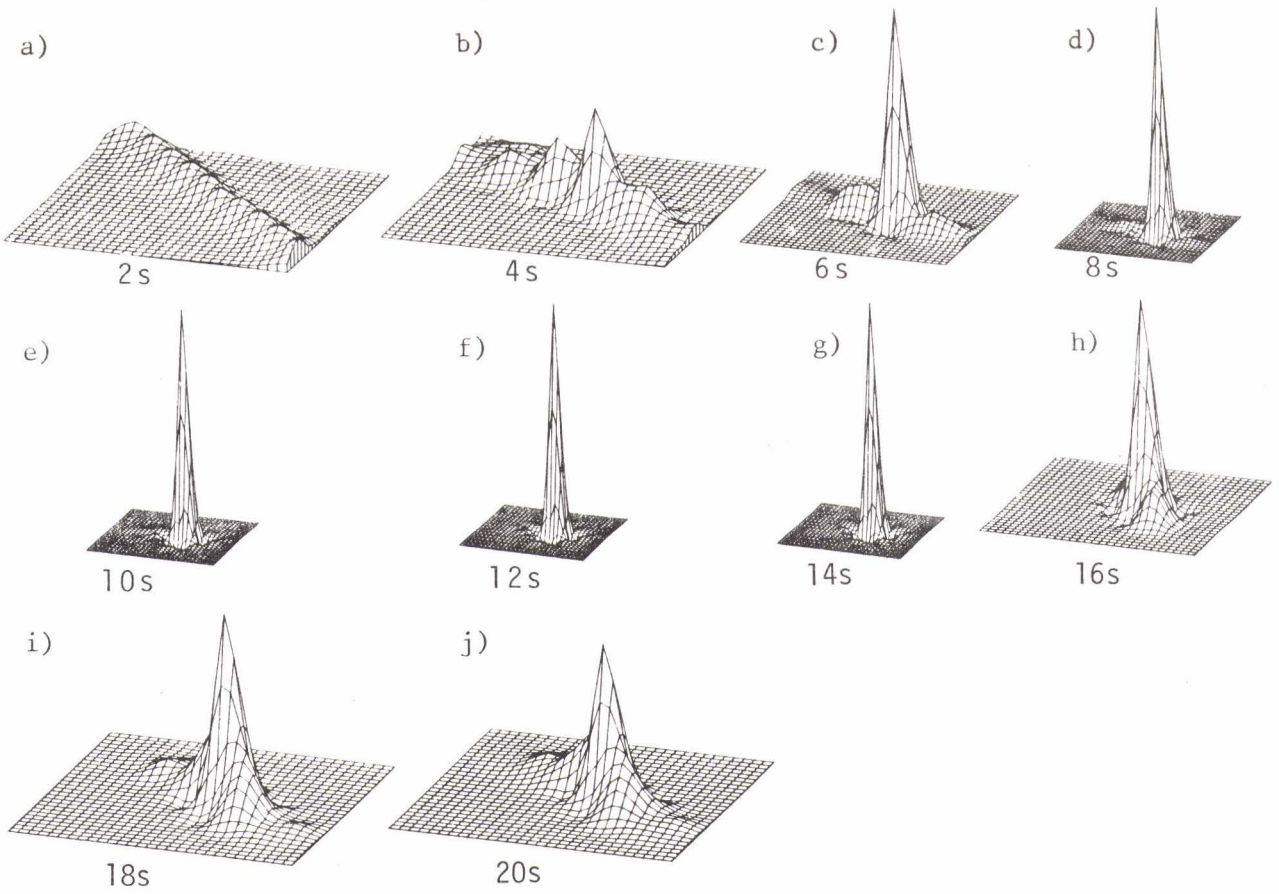
a)
2s
b)
4s
c)
6s
d)
8s
e)
10s
f)
12s
g)
14s
h)
16s
i)
18s
j)
20s

FIG. 7

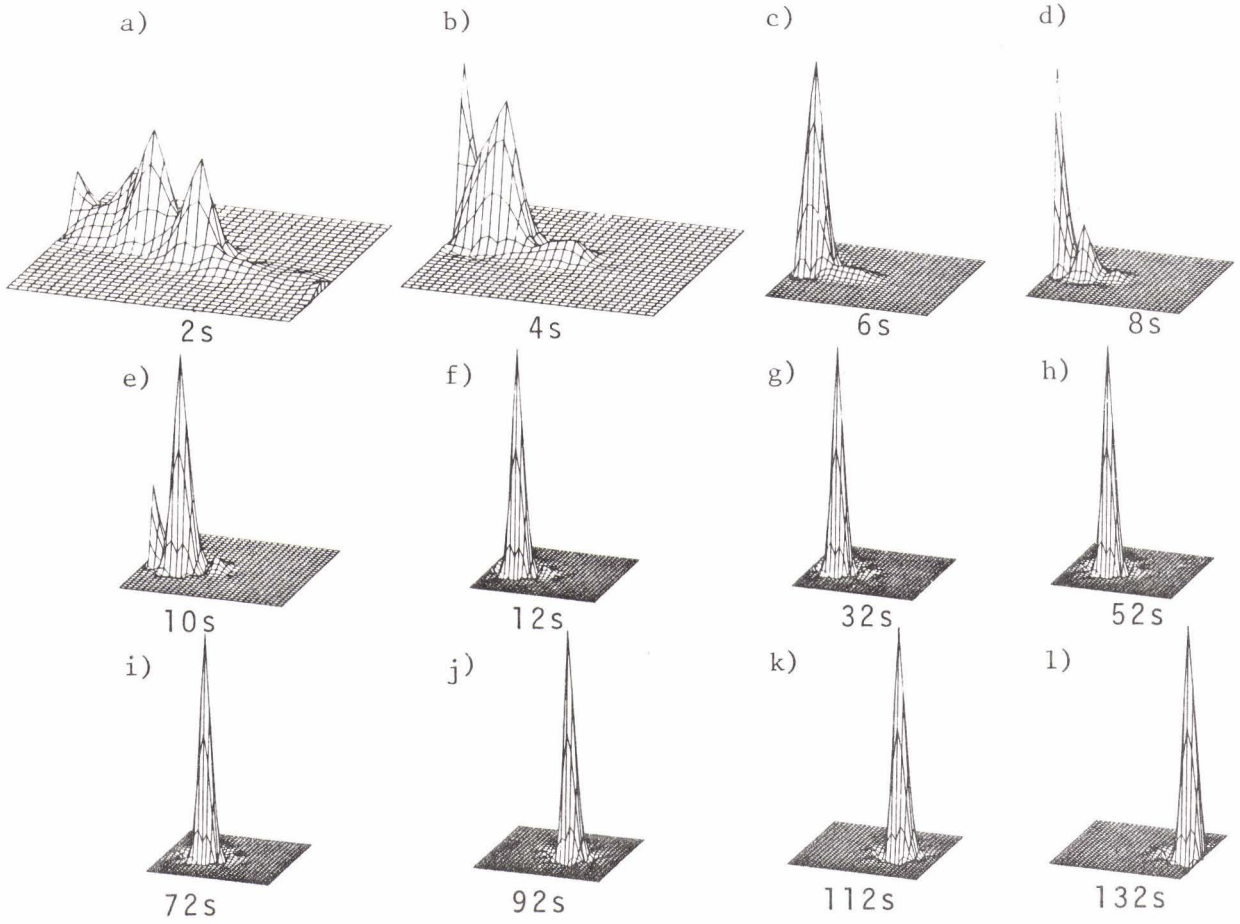
a)
2s
b)
4s
c)
6s
d)
8s
e)
10s
f)
12s
g)
32s
h)
52s
i)
72s
j)
92s
k)
112s
l)
132s

FIG. 8

QUANTIZED CONDITIONAL PROBABILITY DENSITY FUNCTION NUMERICAL VALUES

-106	-131	-134	-147	-164	-194	-203	-220	-302	- ∞	- ∞	2.5
- 81	- 98	- 70	-106	-127	-130	-138	-179	-187	-281	- ∞	2
- 75	- 73	- 69	- 65	- 65	- 97	-115	-115	-122	-171	-281	1.5
- 74	- 48	- 62	- 37	- 61	- 33	- 80	-102	- 96	-106	-151	1
- 66	- 58	- 51	- 42	- 33	- 29	- 33	- 68	- 77	- 84	- 85	0.5
- 94	- 89	- 78	- 73	- 62	- 32	0	- 47	- 65	- 63	- 72	0
-107	- 98	- 90	- 83	- 74	- 63	- 33	- 29	- 36	- 45	- 53	-0.5
-172	-137	-128	-119	-117	- 94	- 65	- 32	- 59	- 39	- 55	-1
-302	-201	-151	-136	-135	-122	-112	- 94	- 65	- 67	- 71	-1.5
- ∞	-303	-216	-201	- 84	-165	-157	-145	-121	-100	- 72	-2
- ∞	- ∞	-333	-240	-234	-225	-194	-175	-162	-150	-134	-2.5
85	86	87	88	89	90	91	92	93	94	95	B \ $\dot{B}$

RATE BINS (degrees / s)

SPATIAL BINS (degrees)

VALUES IN dB

TABLE 1